JJMIE

Volume 18, Number 2, June. 2024
ISSN 1995-6665
Pages 327- 337
https://doi.org/10.59038/jjmie/180206
Editor-in-Chief: Prof. Ali M. Jawarneh

Jordan Journal of Mechanical and Industrial Engineering

Influence of Post-Heat Treatment on the Characteristics of FeCrBMnSi Coating on Stainless Steel 304 Substrate Prepared by Twin Wire Arc Spray (TWAS) Method at Various Stand-off Distance

Agustinus Purna Irawan[1*], Deni Fajar Fitriyana[2*], Januar Parlaungan Siregar [3,4], Tezara Cionita[5], Paula Tjatoerwidya Anggarina[6], Jamiluddin Bin Jaafar[7], Rilo Berdin Taqriban[8], Emilianus Jehadus[9], Janviter Manalu[10]

[1] *Faculty of Engineering, Universitas Tarumanagara, Jakarta 11480, Indonesia*
[2] *Department of Mechanical Engineering, Universitas Negeri Semarang, Kampus Sekaran, Gunungpati, Semarang 50229, Indonesia*
[3] *Faculty of Mechanical & Automotive Engineering Technology, Universiti Malaysia Pahang Al-Sultan Abdullah, Pekan 26600, Malaysia*
[4] *Centre for Automotive Engineering (Automotive Centre), Universiti Malaysia Pahang Al-Sultan Abdullah (UMPSA), Pekan 26600, Pahang, Malaysia*
[5] *Faculty of Engineering and Quantity Surveying, INTI International University, Nilai 71800, Malaysia*
[6] *Faculty of Economics and Business, Universitas Tarumanagara, Jakarta 11480, Indonesia*
[7] *Faculty of Mechanical and Manufacturing Engineering, Universiti Tun Hussein Onn Malaysia, Parit Raja, Batu Pahat 86400, Johor, Malaysia*
[8] *Departement of Mechanical Engineering, Faculty of Engineering, Diponegoro University, Semarang, Jawa Tengah, 50275, Indonesia*
[9] *Universitas Katolik Indonesia Santu Paulus Ruteng, Nusa Tenggara Timur 86511, Indonesia*
[10] *Faculty of Engineering, Universitas Cenderawasih, Kota Jayapura 99358, Indonesia*

Received 29 Feb 2024 *Accepted 13 Apr 2024*

Abstract

Twin wire arc spray (TWAS) is a type of thermal spray coating technology that has been extensively researched to improve the service life and overcome wear, cavitation and corrosion in pump impellers. This study aims to investigate the effect of post-heat treatment on the properties of FeCrBMnSi coatings fabricated by the Twin Wire Arc Spray (TWAS) method on 304 stainless steel substrates with varying stand-off distances. NiAl and FeCrBMnSi were employed as bond coats and top coats in this study. The substrate material was sandblasted before the coating process to achieve a surface roughness of 75–100 µm. The TAFA 9000 Electrical Wire-Arc Spraying machine's voltage (V), current (A), and compressed air pressure (Bar) were set to 28.4; 150; and 5, respectively. The coating operation was performed at 100, 200, and 300 mm stand-off distances. The specimens were then post-heated for 3 hours at 500°C and 700°C in a Thermolyne F6010 Furnace Chamber. The quality of the coating produced in this study was evaluated using thickness, hardness, wear, bond strength, micrography, and SEM (Scanning Electron Microscope) testing. According to the findings of this study, specimens with a stand-off distance of 100 mm and a post-heat treatment temperature of 700ºC produce the best coating qualities when compared to other specimens. This specimen resulted in a percentage of porosity and unmelted material, thickness, hardness, adhesive strength, and total wear rate of 7.1%, 5.53 x 10^{-1} mm, 1460 HV, 24.86 MPa, and 3.8 x10^{-4} mm^3/s, respectively.

Keywords: Twin Wire Arc Spray (TWAS), Pump impeller, 304 stainless steel, Stand-off distance, post-heat treatment.

1. Introduction

Almost every aspect of human existence employs pumps, including surface water treatment and distribution, wastewater treatment, oil and chemical industries, and household water supply [1]–[4]. Typically, these devices consume approximately 20% of the global electrical energy output. Efficiency enhancement initiatives are widely recognized as a critical means of mitigating global environmental impacts and reducing energy consumption, owing to the escalating electricity expenses and the ubiquitous use of pumps in human activities [5]. One of the main components of a pump is the impeller [6], which is often subject to damage such as cavitation, corrosion, and wear [7]. Cavitation is a phenomenon in which the local pressure of a liquid drops below its vapor pressure [8]. Meanwhile, corrosion occurs due to a chemical reaction between the impeller material and the fluid. Impeller blade wear in pumps occurs due to variations in the concentration of sediment contained and the velocity of fluid flow [9].

* Corresponding author e-mail: agustinus@untar.ac.id; deniifa89@mail.unnes.ac.id.

Factors that affect wear include velocity of fluid flow, pressure, surface roughness, and material hardness. Basically, one of the factors affecting wear is the hardness of the component material [10], [11].

According to studies by Silveira et al. [12], cavitation, wear, and corrosion are the primary causes of impeller failure. Cavitation can lead to fatigue damage. Particle erosion in the fluid can lead to wear on the impeller. Meanwhile, exposure to seawater or hot liquids causes corrosion. The occurrence of cavitation, wear, and corrosion on the impeller can be used to determine the escalation in degradation and decrease in performance that happens while various kinds of pumps are in operation [12]. Typically, the efficiency of a pump decreases when it is used to pump water that contains a significant amount of sediment. This results from increased and intense cavitation-abrasive wear on every pump component. Consequently, this results in escalated operational and maintenance expenses. Cavitation and abrasive effects result in pump wear, leading to negative technical and economic outcomes such as decreased energy performance and increased energy consumption [13]. This results in periodic maintenance to mitigate failure effects [14], [15]. The evident outcome is decreased agricultural production due to decreased water availability from the pump [16].

Coating techniques have been extensively implemented across diverse industries to augment the durability and lifetime of components. This is achieved by improving chemical properties, hardness, mechanical properties, tribology, abrasion resistance, and thermal shock resistance [17]–[20]. Besides employing hard metals [21], the thermal spray coating procedure can also be utilized to counteract the erosion and abrasion experienced by pump components [22]. The thermal spray coating process involves heating the material and spraying it onto the surface to be coated, forming a protective layer. A thermal spray method that produces a coating with higher coating hardness and strength, as well as good coating quality with minimal porosity is Twin Wire Arc Spray (TWAS) [23]. This technique is favored due to its minimal equipment and operational costs, as well as its high rate of deposition and mobility. Adjusting the voltage, arc current, type and pressure of the atomizing gas, and stand-off distance, the microstructure of the TWAS coating can be controlled [24], [25]. The TWAS machine's voltage and arc current should be tuned to provide the least variation possible while producing a constant and stable condition. This will facilitate the ongoing melting of the feedstock and allow for the atomization of particles while in motion through a high-velocity gas stream. The gas type and pressure in the TWAS procedure can affect gas density, affecting the size and distribution of particles on the surface of the substrate [25].

The stand-off distance affects the microstructure and mechanical properties of the coating layers. Stand-off distance must be considered to obtain the target thickness of the coating layers [26].

Post heat-treatment of coatings is also important to modify the microstructure and improve the mechanical properties of the coating. Annealing is a post-heat treatment method that uses thermal energy to improve the properties of the deposited coating [27]. Post-heat treatment is one of the most important factors in improving the properties of coatings [28]. Applying post-heat treatment to coating layers can be employed to attain desired target geometries, enhance mechanical properties, and microstructure [25]. Furthermore, post-heat treatment can result in the formation of dense coatings with decreased porosity, which improves the mechanical properties of the coating [29].

Previous studies on the coating of FeCrBMnSi on impeller pumps made of 304 Stainless Steel mainly focused on the influence of process parameters such as stand-off distance, air pressure, and post-heat treatment on the microstructure, adhesion strength, mechanical properties, and mass loss of the coating layer. There is limited research on the various combinations of TWAS parameters, such as post-heat treatment and stand-off distance, which can improve the characteristics of coating layers, including microstructure, thickness, adhesion strength, hardness, and wear resistance. Therefore, this research was conducted to determine the effect of post-heat treatment on the characteristics of FeCrBMnSi coatings produced using the Twin Wire Arc Spray (TWAS) method on 304 stainless steel substrates with different stand-off distances. The post-heat treatment in this study is intended to diminish residual thermal stresses in the FeCrBMnSi coating, refine its grain structure, homogenize the microstructure, enhance mechanical properties, improve wear resistance, and enhance the adhesion of the coating layer. The results can help improve the properties of FeCrBMnSi coatings by using post-heat treatment.

2. Materials and Methods

2.1. Materials

In this research, 304 stainless steel was used as the raw material for the pump impeller specimen. The chemical composition of the 304 stainless steel used in this study is detailed in Table 1 [24]. The 304 stainless steel is a material with good resistance to corrosion, with a density and modulus of elasticity of 7.9 g/cm^3, and 180 GPa, respectively [30]. In this research, bond coat material is used to strengthen the bond between the coating layer and the substrate. The type of bond coat used is TAFA 75B (Ni-Al). This product has a melting point of 2642°F (1450°C), with Ni and Al contents of 95% and 5%, respectively [31].

Table 1. 304 stainless steel's chemical composition

Element	Percentage (%)
C	0.08
Mn	2
P	0.045
S	0.3
Si	1
Cr	18
Ni	8
Fe	Balance

This study used TAFA 95 MXC or FeCrBMnSi as the top coat material, with its chemical composition provided in Table 2 [32]. The wire size and melting point of this material are 1.6 mm and 1204ºC [32]. TAFA 95B and TAFA 95 MXC used in this study were obtained from TAFA Incorporated, Concord, New Hampshire, USA.

Table 2. TAFA 95 MXC chemical composition

Element	Percentage (%)
Si	1.7
Cr	28
Mn	2
B	3.7
Fe	64.6

2.2. Fabrication of Specimen and Testing

This research uses a 304 stainless steel plate as a substrate with a size of 100 mm x 100 mm x 6 mm (Figure 1). Sandblasting was performed using aluminum oxide with a mesh size of 24 to obtain an average surface roughness on the substrate of 75 − 100 µm. Substrate preparation and blasting equipment followed NACE 2 or SSPC SP-10 (Near White Blasting) standards. The sandblasting process used a Norblast Sandblasting machine with type NOB35CE, form Norexco SA, Ville-la Grand, France.

Figure 1. Substrate materials (dimensions in mm)

The coating process in this study used the Twin Wire Electrical Arc-Spraying method with a TAFA 9000 Electrical Wire-Arc Spraying machine from TAFA Incorporated, Concord, New Hampshire, United States of America (Figure 2) with detailed specifications shown in Table 3.

The coating process was carried out using the TAFA 9000 Electric Wire Arc Spraying machine by setting the voltage (V), current (A), and compressed air pressure (Bar) to 28.4; 150; and 5, respectively. In this study, the coating process on the substrate was carried out with stand-off distances of 100 mm, 200 mm, and 300 mm. Post heat treatment was carried out after the coating process to increase the hardness of the coated parts. To accomplish maximum hardness, this post-heat treatment is performed at 500°C and 700°C for 3 hours and then allowed to cool to room temperature in the furnace [33].

Figure 2. PRAXAIR TAFA 9000 Arc-Spray Machine

Table 3. PRAXAIR TAFA 9000 Arc-Spray Machine specifications

Parameters	Value
Input ampere	< 23 A
Input voltage	200 V
Input frequency	50−60 Hz
Output ampere	100−200 A
Output voltage	18−30 V
Spraying Air pressure	3−5 Bar
Wire size	1.6−2.5 mm

The quality of the coating produced in this study was evaluated using thickness, hardness, wear, bond strength, micrography, and SEM (Scanning Electron Microscope) testing. The tests will be carried out on specimens that have been coated with post-heat treatment and on specimens that have been coated without post-heat treatment. Scanning Electron Microscope (SEM) (Hitachi High-Tech, Toranomon, Minato-ku, Tokyo, Japan) was used to observe the morphology of the specimen. SEM images were then analysed with ImageJ software to determine the amount of porosity and unmelted material in each specimen [24], [34]. The construction of the coating layer was observed using a LOM (light optical microscope) with an Olympus U-MSSP4 (Evident Corporation, Shinjuku-ku, Tokyo, Japan), which refers to the ASTM E3 standard in 2007. The results of this test will be analyzed using ImageJ software to estimate the thickness of the produced coating layer.

Hardness testing of the coating layer was carried out using Mitutoyo Micro Vickers Hardness Testing Machines HM-210 series (Mitutoyo Corporation, Kanagawa, Japan) regarding ASTM E92-82 standard in 2003. This test is carried out with an indenter loading of 0.5 kgf for 10 seconds. The pull-off bonding method was performed with the standard used was ASTM D-4541. A 20 mm diameter dolly was adhered to the surface of the coated specimen to conduct the test. This study utilized Araldite adhesive to adhere the surfaces of the specimen and dolly together. A 24-hour ageing process was undertaken to provide excellent

adhesion between the dolly and the surface of the specimen. The test process utilized a PosiTest AT-M Adhesion Tester (DeFelsko, New York, USA) to apply force on the dolly attached to the surface of the specimen.

Wear tests were carried out according to ASTM G99-95A using the pin-on-disc method [35]–[38].

The coated specimens were sectioned using the Everising S-12H machine to produce specimens with dimensions of 10 mm x 10 mm x 6 mm. These specimens were then joined to the pins on the pin-on-disc machine. The abrasive material used as a disc in this study is silica carbide paper. The pin-on-disc test was performed 10,000 cycles with a disc rotation speed of 100 rpm and a given load of 300 g. In this study, the abrasive material was changed every 500 cycles. The wear rate calculations are based on prior research [24], [34].

3. Results and Discussions

Figure 3 depicts the results of an SEM test with 4000x magnifications on one of the specimens. Porosity, unmelted material, and oxides are visible in SEM images. This phenomenon can be found in all specimens produced, both with and without post-heat treatment.

ImageJ software was used to calculate the percentage of porosity and unmelted material. Figure 4 illustrates the use of ImageJ software to estimate the percentage of porosity and unmelted material in SEM images of one of the specimens produced in this study. This calculation is based on the method used in previous studies [24], [34].

The effect of stand-off distance and post-heat treatment on the percentage of porosity and unmelted material is shown in Figure 5. This study illustrates that in specimens that do not undergo post-hardening treatment, the presence of porosity and unmelted material increases as the stand-off distance increases from 100 mm to 200 mm.

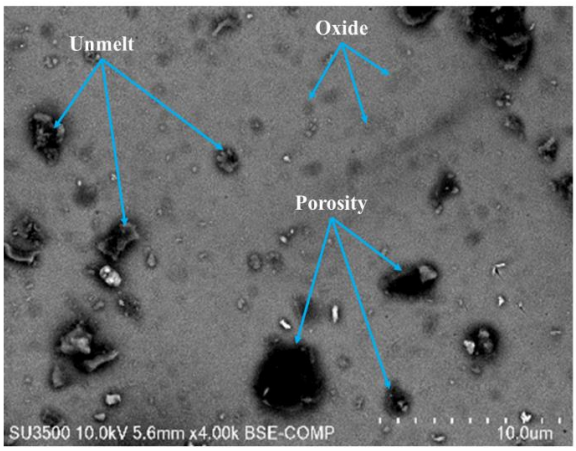

Figure 3. Morphology of the coating layer obtained on the specimen

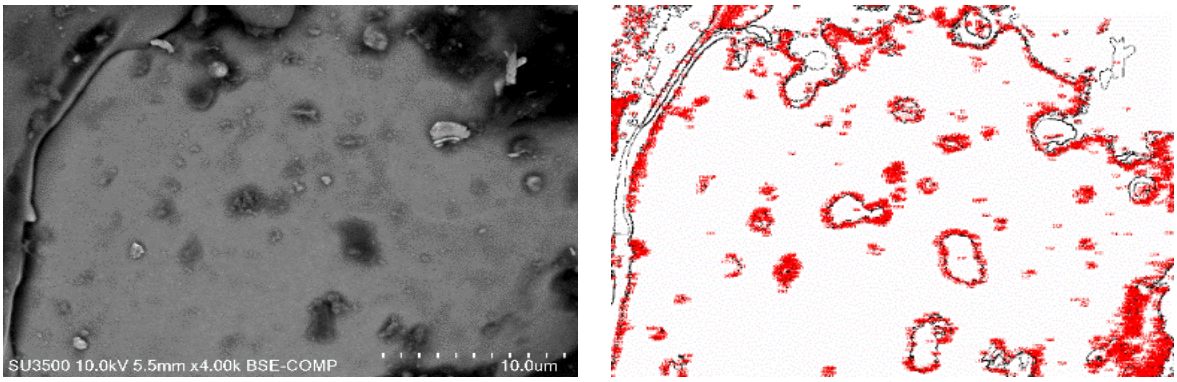

(a) (b)

Figure 4. Percentage measurement of porosity and unmelted material using ImageJ software. (a) SEM Images and, (b) ImageJ analysis results

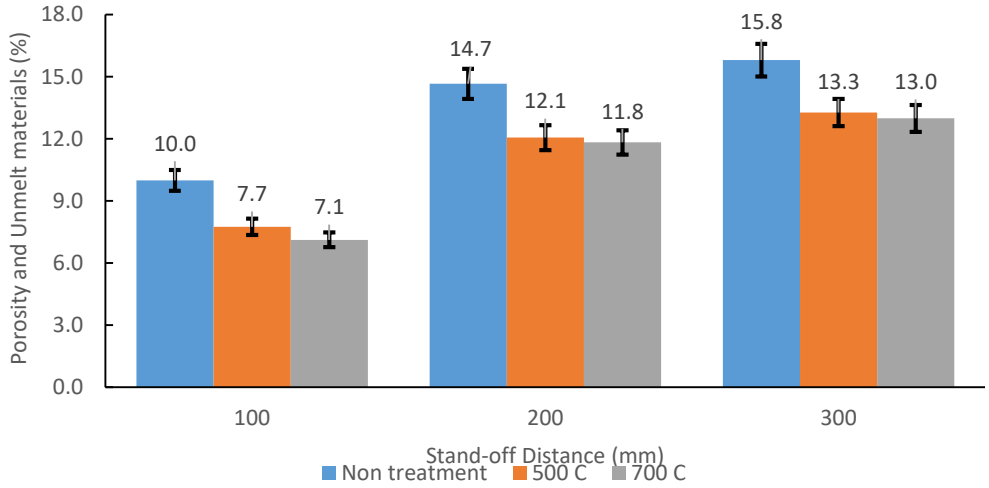

Figure 5. The effect of stand-off distance and post-annealing treatment on the percentage of porosity and unmelted material

However, there is a slight increase in porosity and unmelted material when the stand-off distance exceeds 200 mm. Increasing the distance between the object and the heat source (stand-off) leads to higher porosity and unmelted material produced. Increasing the stand-off distance results in a prolonged cooling process for the melted coating material as it moves towards the substrate. This causes the melted coating material to adhere to the substrate when it is in a low temperature or cooled state. This results in reduced wettability of the droplets, which leads to the formation of an imperfect coating layer. As a result, greater porosity and non-melting material is produced when the stand-off length is increased [24]. The smallest percentage of porosity and unmelted material is found in specimens coated with a stand-off distance of 100 mm and post-heat treatment at 700ºC. This specimen produces a percentage of porosity and unmelted material of 7.1%. Meanwhile, the largest percentage of porosity and unmelted material was found in the coated specimen with a stand-off distance of 300 mm without post-heat treatment. This specimen produces a percentage of porosity and unmelted material of 15.8%. The results of this study show that post-heat treatment reduces the percentage of porosity and unmelted material at all variations of stand-off distance. Furthermore, the higher the post-heat treatment temperature used, the less percentage of porosity and unmelted material there is in the coating layers.

The percentage of porosity and unmelted material increases as the stand-off distance increases [24]. Meanwhile, an increase in the post-heat treatment temperature used causes the percentage of porosity and unmelted material to decrease. This happens because as the post-heat treatment temperature rises and the stand-off distance decreases, there is an increase in particle transportation from high concentration to low concentration to fill the void. Consequently, the percentage of unmelted material and porosity in the coating layer decreases [39], [40].

The findings of this study indicate that the percentage of porosity and unmelted material rises as the stand-off distance increases. Nevertheless, when the temperature increased throughout the post-heat treatment procedure, the amount of porosity and unmelt in the coating layer reduced across all stand-off distances. This phenomenon arises due to the elevation of the post-heat temperature, which creates a more uniform microstructure. Consequently, this reduces the presence of pores and enhances the solidification of the coating layer. Moreover, raising the temperature of the post-heat treatment promotes a more efficient re-melting process. This will decrease the quantity of presence and minimize pores while establishing a strong metallurgical connection between the coating layers and the substrate. The study's findings are consistent with research by Fu Bin-You et al. (2009), which found that the percentage of porosity and unmelt increases with increasing stand-off distance. However, with increasing annealing temperatures, the percentage of porosity decreases [41]. Additionally, Cheng et al. [42] found that increasing the annealing temperature can decrease porosity and increase hardness. This occurs because increasing the annealing temperature causes an increase in microstructure homogeneity, reduction of porosity and higher solidification of the coating layer [42]. Based on a study conducted by Daram et al., [43] the re-melting process during post-annealing treatment can eliminate pores and create a strong metallurgical bond between the coating and the substrate. The reduction in porosity after post-heat treatment occurs because the microstructure contains more oxide phases in the intersplat boundary layer, resulting in a reduction in the number of open pores [43].

According to Zhou et al. [44] research, increasing the heat treatment temperature causes recrystallization in the coating layers. The recrystallization process leads to the surface of the particles blurring and disappearing, numerous pores closing, and the coating's porosity decreasing significantly [44].

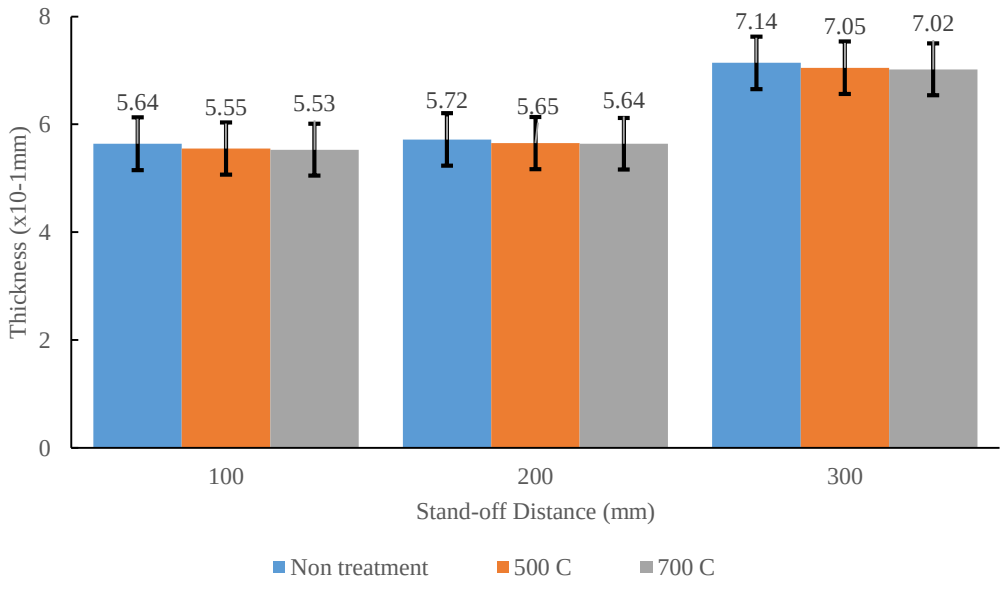

Figure 6. The effect of stand-off distance and post-annealing treatment on coating layer thickness

Figure 6 depicts the effect of stand-off distance and post-heat treatment on coating layer thickness. The results of this study show that specimens without post-heat treatment with a stand-off distance of 300 mm have the thickest coating layer. The coating layer on this specimen is 0.714 mm thick. The specimen's thinnest coating layer was then discovered with a stand-off distance of 100mm and a post-heat treatment at 700ºC, yielding a coating thickness of 0.553 mm.

The results of this study show that increasing the temperature in the post-heat treatment causes a decrease in the thickness of the coating layer in all variations of the stand-off distance. The percentage of unmelted material and porosity have a significant impact on the coating layer thickness [45]. According to the findings of this study, the thickest coating layer is found on specimens with the highest percentage of porosity and unmelted material. In contrast, the thinnest coating layer is found in specimens with the lowest percentage of porosity and unmelted material. As the percentage of porosity and unmelted material decreases, the interlamellar bond strengthens, resulting in a thinner coating layer [43]. These results are in accordance with research conducted by Daram et al. [43] and Nayak et al. [46]. Their results show that increasing the amount of porosity causes the thickness of the coating layer to increase [43], [46]. Furthermore, the post heat treatment temperature also had a significant impact. When the temperature was increased from 500°C to 700°C, the coating thickness tended to increase or stabilize. High temperature during post heat treatment can improve the adhesion of coating particles, resulting in a denser and more stable coating [47]–[49].

Twin Wire Arc spray coating followed by post-heat treatment with different temperatures in this study causes the formed coating to undergo structural changes that affect the thickness and properties of the coating layer. The effect of stand-off distance and post-heat treatment on the hardness of the coating layer is shown in Figure 7. The results of this study show that specimens coated instead of post-heat treatment have a hardness of 800-1200 HV. The specimens coated and post-heat treatment at 500°C had a hardness ranging from 1000 to 1400 HV.

Coated and post-heat treatment at 700°C specimens have a hardness range of 1100-1500 HV. The hardest specimens were coated with a stand-off distance of 100 mm and post-heat treatment at 700°C. This specimen produced a hardness of 1460 HV. While specimens coated with a stand-off distance of 300 mm and without post-heat treatment achieved the lowest hardness of 893 HV. The results of this study show that specimens with the highest hardness are found in specimens that have the smallest percentage of porosity and unmelted material. While specimens with the lowest hardness are found in specimens that have the highest percentage of porosity and unmelted material. According to the findings of this study, increasing the temperature in the post-heat treatment causes an increase in the hardness of the coating layer at all stand-off distance variations.

The coating properties are greatly influenced by porosity [50]–[52]. The hardness of the coating layer increases as the percentage of porosity and unmelted material decreases. The presence of unmelted or compacted particles entrapped within the coating is generally associated with higher porosity. Porosity causes inadequate coating cohesion and reduces the ability to endure indentation loads, resulting in a decrease in hardness. Furthermore, porosity in the coating can result in rising corrosion rates and wear [50]–[52]. The porosity of a coating is inversely related to its hardness. The hardness of the coating increases as the porosity decreases. A study on HVOF-sprayed $WC_{10}Co_4Cr$ coatings, for example, discovered that optimising process parameters resulted in coatings with low porosity (0.2 Vol. Percentage) and maximum hardness (1325.26 HVx) [53]. Furthermore, a study found that the presence of the lowest porosity causes the Fe-based amorphous coatings to have the highest hardness [50]. These findings show that decreasing porosity leads to an increase in coating hardness.

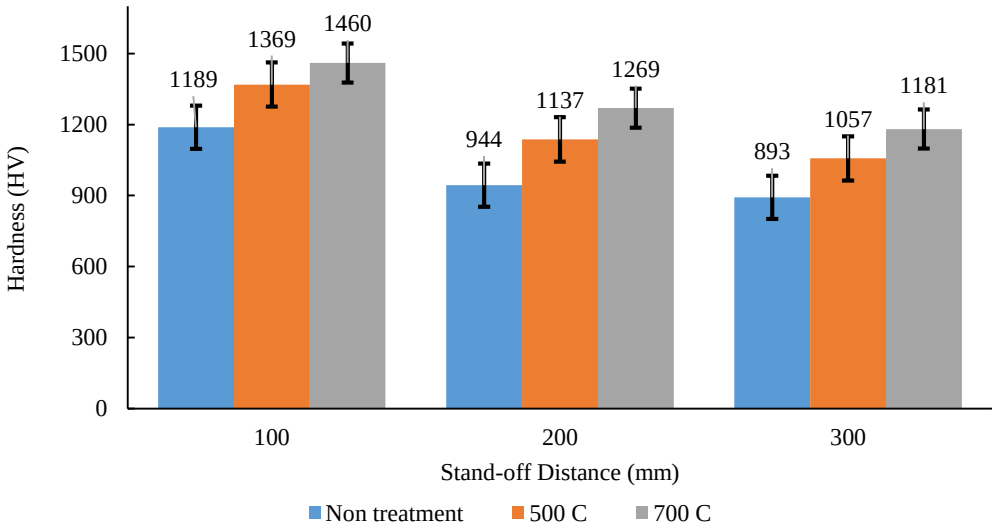

Figure 7. The effect of stand-off distance and post-annealing on the hardness of the coating layer

The greater the stand-off distance, the oxide content attached to the coating increases, the increase in the value of oxide content will make the hardness value of the coating tend to decrease [54]. In addition, the increase in post-heat treatment temperature made the coating layer increase in hardness value. This is due to a decrease in tensile residual stress in the coating layer [55], [56]. According to Zhang et al. [57] study findings, high-temperature annealing (>700°C) results in a homogeneous microstructure with low porosity. This will increase the number of microcracks, which will increase hardness as well as fracture toughness [57]. The same phenomenon was also found in research conducted by Dhiflaoui et al. [58] and Kosasih et al. [59]. Their results show that the increase in annealing temperature improves the hardness.

Figure 8 shows the effect of stand-off distance and post-heat treatment temperature on adhesive strength of coating layers. Pull off bonding test conducted in this study is used to determine the amount of adhesive strength between the coating layer and the substrate.

The results of this study show that the highest adhesive strength is found in specimens coated with a stand-off distance of 100 mm and post-heat treatment at 700°C. This specimen produced a hardness of 24.86 MPa. Meanwhile, specimens coated with a stand-off distance of 300 mm and without post-heat treatment produced the lowest adhesive strength of 18.52 MPa. In general, the adhesive strength produced in this study meets the ASM standard for twin wire arc spray, which is 10−40 MPa [60].

The results of this study indicate that specimens with the highest adhesive strength are found in specimens that have the smallest percentage of porosity and unmelted material. While specimens with the lowest adhesive strength are found in specimens that have the highest percentage of porosity and unmelted material. According to the findings of this study, an increase in temperature in the post-heat treatment led to an increase in the adhesive strength of the coating layers at all variations of stand-off distance.

According to this study, increasing the stand-off distance will reduce the adhesion strength of the coating layer to the substrate due to the greater value of porosity and unmelt contained in the coating layer [61]. In contrast, the specimens with 500°C and 700°C post-heat treatment, the adhesion value tended to increase compared to the coating without post-heat treatment. This occurs because the annealing process results in a decrease in percentage of porosity and unmelt materials, thus increasing the adhesion of the coating [62]. Increased porosity can result in reduced adhesion between the coating layer and the substrate. This is caused by poor mechanical and chemical adhesion, as well as incomplete pore filling. As a result, interlocking and adhesion are ineffective.

According to other reports, the higher the percentage of porosity and unmelted material, the lower the adhesive strength of the coating. Porosity in the coating reduces bond strength due to pores giving pathways for crack propagation. Furthermore, the presence of porosity leads to the coating layer delaminating from the substrate. When porosity is reduced, the coating has an increased density and an additional continuous structure, which strengthens the bond between the coating and the substrate [63]. The coating layer's porosity is defined as the existence of voids, pores, or holes in it. The coating's bonding strength increases with decreasing porosity.

This is because reduced porosity indicates fewer coating defects, which may reduce the bonding strength. The bonding strength of a coating can be significantly affected by the presence of numerous small particles and unmelted materials caused by porosity in the coating. Thus, lowering the coating's pore number and other defects could assist in improving the coating's adhesive strength [64].

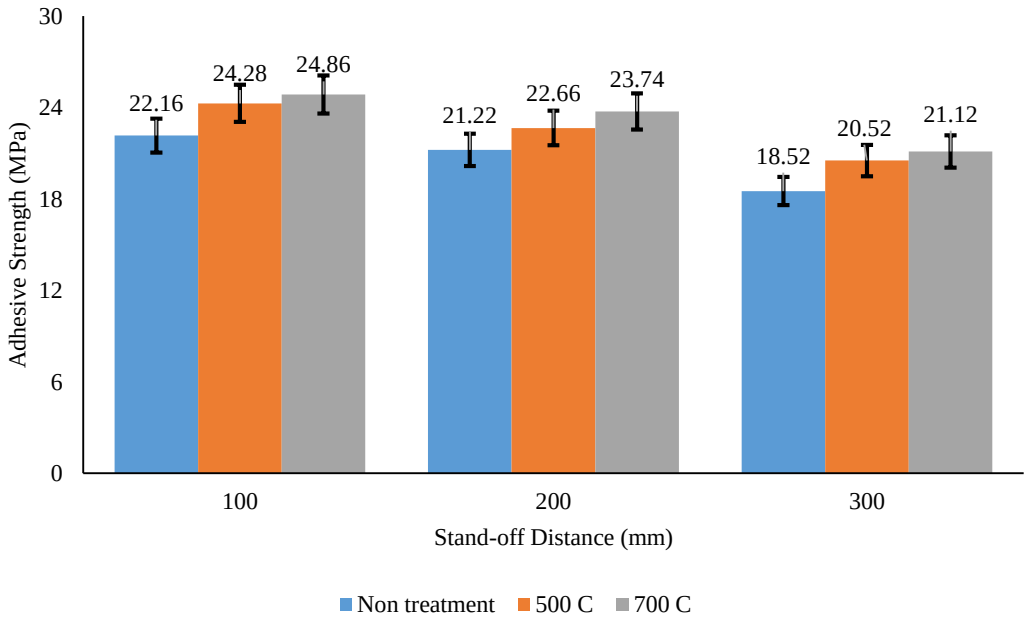

Figure 8. The effect of stand-off distance and post-annealing temperature on coating adhesive strength

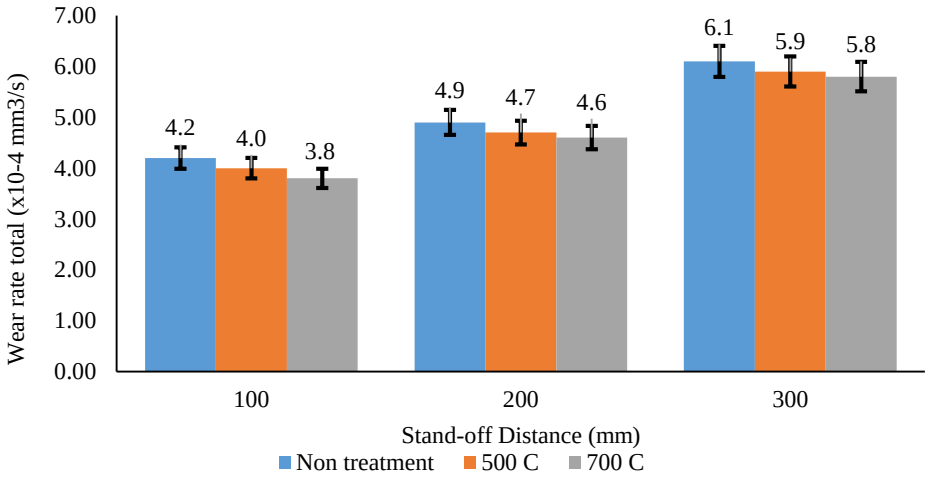

Figure 9. The effect of stand-off distance and post-annealing temperature on coating wear resistance

The effect of stand-off distance and post-heat treatment temperature on the wear rate of the coating layer is shown in Figure 9. The results of this study show that the lowest wear rate was found on specimens coated with a stand-off distance of 100 mm and annealed at 700°C. This specimen produced a wear rate of 3.8 x 10^{-4} mm^3/s.

Meanwhile, specimens coated with a stand-off distance of 300 mm and without annealing produced the highest wear rate of 6.1 x 10^{-4} mm^3/s. According to the findings of this study, increasing the temperature in the post-heat treatment causes a decrease in the wear rate of the coating layer at all variations of the stand-off distance.

In other words, increasing the temperature in the post-heat treatment led to an increase in the wear resistance of the coating layer at all variations of the stand-off distance. In the study of Zhu et al. [65], the wear resistance of AlCrTiSiN coating made by arc ion plating was improved after annealing treatment [65]. Based on the findings in this study, the specimen with the highest wear rate is found in the specimen that has the highest percentage of porosity and unmelted material. While the specimen with the lowest wear rate is found in the specimen that has the lowest percentage of porosity and unmelted material. Higher porosity of materials causes increased wear rates, as confirmed by a research study by Lavrys et al. [66]. Pores act as stress raisers and are a source of crack propagation, which can cause damage to a material system [66].

The wear rate obtained in this study is strongly related to the hardness and thickness of the coating layer, in addition to the percentage of porosity and unmelted material. The results revealed that the specimen with the highest wear rate had the lowest hardness and thickest coating thickness. The specimen with the lowest wear rate was discovered to have the highest hardness and thin coating thickness. According to the findings of this study, the wear resistance of coatings is dependent on the hardness and thickness produced. The findings of this study are consistent with the findings of Zhai et al. [66]. According to their findings, the hardness and thickness of the coating layer determine wear resistance and friction coefficient.

Hardness is directly related to wear resistance; hard materials wear less than soft ones. Thickness, on the other hand, is one of the factors influencing abrasive wear resistance as a result of mass sliding friction. Gas nitriding (GN) and combined deformation-diffusion treatment (DDT) of porous titanium lead to the creation of a nitride layer accompanied by a diffusion zone underlying it. Based on XRD examination, the intensity of the nitride phase is greater for titanium after DDT than after GN. This suggests that a thicker surface nitride layer is formed due to DDT. As a result, the surface microhardness is greater after DDT than it is after GN. Therefore, porous titanium with GN and DDT exhibits superior wear resistance compared to ball burnishing (BB) products in these specific tribo interaction settings [66].

Decreasing the hardness of the coating will make the wear resistance of the coating material tend to be low [35], [67]–[73]. A increase in stand-off distance results in a decrease in hardness value which will make the mass loss and wear rate of the specimen tend to be high [24], [28]. This can be improved by annealing after the coating process is finished. This study demonstrates that increasing the post-heat treatment temperature reduces the wear rate due to the increased hardness of the coating layer [74], [75]. Furthermore, at all stand-off distance variations, the wear rate on specimens without post-heat treatment treatment is higher than the wear rate on specimens with post-heat treatment.

Conclusions

The application of Twin Wire Arc Spray (TWAS) as a coating technique to prevent wear, cavitation, and corrosion in pump impellers is discussed in this study. The effects of post-heat treatment temperature and stand-off distance on the coating properties are the primary focus of this study. The coating was characterized by several tests and analyses, including microstructure, hardness, wear, thickness, adhesive strength and SEM.

The results of this investigation demonstrate that as stand-off distance increases, correspondingly increases the percentage of porosity and unmelted material. Nevertheless, after post-heat treatment, the percentage of porosity and unmelted material decreased. The findings of this investigation show that at all stand-off distance variations, an increase in temperature during the post-heat treatment decreased the percentage of porosity and unmelted material in the coating layers. An increase in the percentage of porosity and unmelted material leads to an increase in the thickness of the resulting coating layer. Furthermore, an

increase in the percentage of porosity and unmelted material leads to a decrease in hardness, wear resistance, and adhesion strength of the coating layer.

In comparison to other specimens, specimens coated with a variation of 100 mm stand-off distance and post-heat treatment at 700°C have the lowest percentage of porosity and unmelted material. As a result, the coating layer in this specimen has superior thickness, hardness, adhesive strength, and wear resistance than the other specimens. The percentage of porosity and unmelted material, thickness, hardness, adhesive strength, and wear rate total of this specimen are 7.1%, 5.53 x 10^{-1} mm, 1460 HV, 24.86 MPa, and 3.8 x10^{-4} mm^3/s, respectively**.** At a stand-off distance of 100 mm, specimens treated with post-heat treatment at 700°C decreased porosity and unmelted material (%) and thickness (mm) by 29% and 2% compared to specimens without post-heat treatment. Furthermore, the hardness and adhesive strength of these specimens increased by 23% and 17%, respectively. In addition, the specimen with post-heat treatment at 700oC showed the best wear resistance. This is indicated by a 10% decrease in total wear rate compared to specimens without post-heat treatment.

Acknowledgements

The authors would like to express their gratitude for the financial support received Universitas Tarumanagara through the Block Grant Research Assignment Scheme under the International Research Scheme with number of 011-Int-BGRA-I-KLPPM/UNTAR/XII/2022.

Conflicts of interest

The authors declare that they have no conflict of interest.

References

[1] A. Ali, M. Al_Soud, E. Abdallah, and S. Addallah, “Water Pumping System with PLC and Frequency Control”, Jordan Journal of Mechanical and Industrial Engineering, vol. 3, no. 3, 2009, pp. 216–221. https://jjmie.hu.edu.jo/files/v3n3/8.pdf

[2] M. Abu-Aligah, “Design of photovoltaic water pumping system and compare it with diesel powered pump”, Jordan Journal of Mechanical and Industrial Engineering, vol. 5, no. 3, 2011, pp. 273–280. https://jjmie.hu.edu.jo/files/v5n3/jjmie 252-09.pdf

[3] J. Alaydi, “Mathematical modeling for pump controlled system of hydraulic drive unit of single bucket excavator digging mechanism”, Jordan Journal of Mechanical and Industrial Engineering, vol. 2, no. 3, 2008, pp. 157–162. http://www.jjmie.hu.edu.jo/files/JJMIE-V2-N3-press/6(42-47).pdf

[4] N. Beithou, M. Abu Hilal, and I. Abu-Alshaikh, “Thermal analysis of discrete water supply in domestic hot water storage tank”, Jordan Journal of Mechanical and Industrial Engineering, vol. 5, no. 1, 2011, pp. 29–32. https://jjmie.hu.edu.jo/files/v5n1/JJMIE-5.pdf

[5] P. A. Deshmukh, K. D. Deshmukh, and N. A. Mandhare, “Performance enhancement of centrifugal pump by minimizing casing losses using coating”, SN Applied Sciences, vol. 2, no. 2, 2020, pp. 1–10. doi: 10.1007/s42452-020-2042-7.

[6] W.G. Li, “Inverse Design of Impeller Blade of Centrifugal Pump with a Singularity Method”, Jordan Journal of Mechanical and Industrial Engineering, vol. 5, no. 2, 2011, pp. 119–128. https://jjmie.hu.edu.jo/files/v5n2/JJMIE-52-10%20(China)(2).pdf.

[7] E. Kauczor, Damaged Impellers in a Rotary Pump. In: ASM Failure Analysis Case Histories: Failure Modes and Mechanisms, ASM International, 2019. doi: 10.31399/asm.fach.modes.c9001202.

[8] S. Xu, Y. Qiao, X. Liu, C. C. Church, and M. Wan. Fundamentals of Cavitation. In Cavitation in Biomedicine, Dordrecht: Springer Netherlands; 2015, pp. 1–46. doi: 10.1007/978-94-017-7255-6_1.

[9] R. O. P. Serrano, L. P. Santos, E. M. de F. Viana, M. A. Pinto, and C. B. Martinez, “Case study: Effects of sediment concentration on the wear of fluvial water pump impellers on Brazil’s Acre River”, Wear, vol. 408–409, 2018, pp. 131–137. doi: 10.1016/j.wear.2018.04.018.

[10] D. K. Dwivedi. Materials for Controlling the Wear. In Surface Engineering, New Delhi: Springer India, 2018, pp. 45–72. doi: 10.1007/978-81-322-3779-2_3.

[11] Y. Kumar, “An Overview of Wear and How to Improve Wear Resistance”, International Journal for Research in Applied Science and Engineering Technology, vol. 9, no. VI, 2021, pp. 4629–4634. doi: 10.22214/ijraset.2021.36159.

[12] N. Silveira, A. Meghoe, and T. Tinga, “Integration of multiple failure mechanisms in a life assessment method for centrifugal pump impellers”, Advances in Mechanical Engineering, vol. 15, no. 6, 2023, pp. 1–18. doi: 10.1177/16878132231175755.

[13] V.R. Rao, N.Ramanaiah, and M.M.M.Sarcar, “Optimization of Volumetric Wear Rate Of AA7075-TiC Metal Matrix Composite by Using Taguchi Technique”, Jordan Journal of Mechanical and Industrial Engineering, vol. 10, no. 3, 2016, pp. 189–198. https://jjmie.hu.edu.jo/vol%2010-3/JJMIE-53-16-F-4.pdf

[14] I. H. Afefy, A. Mohib, A. M. El-kamash, and M. A. Mahmoud, “A new framework of reliability centered maintenance”, Jordan Journal of Mechanical and Industrial Engineering, vol. 13, no. 3, 2019, pp. 175–190. https://jjmie.hu.edu.jo/vol-13-3/88-19-01.pdf

[15] J. Abbas, A. Al-habaibeh, and D. Su, “The Effect of Tool Fixturing Quality on the Design of Condition”, Jordan Journal of Mechanical and Industrial Engineering, vol. 5, no. 1, 2011, pp. 17–22. https://jjmie.hu.edu.jo/files/v5n1/JJMIE-3.pdf.

[16] M. Mamazhonov, B. Shakirov, B. Matyakubov, and A. Makhmudov, “Polymer materials used to reduce waterjet wear of pump parts”, Journal of Physics: Conference Series, vol. 2176, no. 1, 2022, pp. 1–5. doi: 10.1088/1742-6596/2176/1/012048.

[17] V. Chawla, D. Puri, S. Prakash, and B. Sidhu, “Salt Fog Corrosion Behavior of Nanostructured TiAlN and AlCrN Hard Coatings on ASTM-SA213-T-22 Boiler Steel”, Jordan Journal of Mechanical and Industrial Engineering, vol. 5, no. 3, 2011, pp. 247–253. https://jjmie.hu.edu.jo/files/v5n3/JJMIE%20123-09.pdf.

[18] B. Skoric, D. Kakas, and A. Miletic, “Synthesis of hard coatings and nano modification with ion implantation”, Jordan Journal of Mechanical and Industrial Engineering, vol. 5, no. 1, 2011, pp. 33–38. https://jjmie.hu.edu.jo/files/v5n1/JJMIE-6.pdf.

[19] S. Sarkar, R. Mandal, N. Mondal, S. Chaudhuri, T. Mandal, and G. Majumdar, “Modelling and Prediction of Micro-hardness of Electroless Ni-P coatings Using Response Surface Methodology and Fuzzy Logic”, Jordan Journal of Mechanical and Industrial Engineering, vol. 16, no. 5, 2022. pp. 729–742. https://jjmie.hu.edu.jo/vol16-5/07-JJMIE-189-22.pdf.

[20] F. Zeqiri and B. Fejzaj, “Experimental Research and Mathematical Modeling of Parameters”, Jordan Journal of Mechanical and Industrial Engineering, vol. 16, no. 5, 2022, pp. 787–792. https://jjmie.hu.edu.jo/vol16-5/12-JJMIE-224-22.pdf.

[21] N. Pokharel, A. Ghimire, B. Thapa, and B. S. Thapa, "Wear in centrifugal pumps with causes, effects and remedies: A Review", IOP Conference Series: Earth and Environmental Science., vol. 1037, no. 1, 2022, pp. 1–20. doi: 10.1088/1755-1315/1037/1/012042.

[22] J. Thorne, T., Kennedy, "Increasing Pump Life & Performance in Water & Wastewater Applications", Pumps & Systems, 2021. https://www.pumpsandsystems.com/increasing-pump-life-performance-water-wastewater-applications (accessed Jan. 19, 2024).

[23] Z. Nurisna, S. Anggoro, and H. Nur Mujtahid, "Physical and Mechanical Properties of Twin-Wire Arc Spray and Wire Flame Spray Coating on Carbon Steel Surface", Materials Science Forum, vol. 1057, 2022, pp. 235–239, doi: 10.4028/p-z698i0.

[24] D. F. Fitriyana, W. Caesarendra, S. Nugroho, G. D. Haryadi, M. A. Herawan, M. Rizal, R. Ismail, "The Effect of Compressed Air Pressure and Stand-off Distance on the Twin Wire Arc Spray (TWAS) Coating for Pump Impeller from AISI 304 Stainless Steel", Springer Proceedings in Physics, vol. 242, 2020, pp. 119–130. doi: 10.1007/978-981-15-2294-9_11.

[25] B. Kuhlenkötter, T. Glaser, S. Fahle, S. Husmann, M. Abdulgader, and W. Tillmann, "Investigation of compaction by ring rolling on thermal sprayed coatings", Procedia Manufacturing, vol. 50, 2020, pp. 192–198. doi: 10.1016/j.promfg.2020.08.036.

[26] W. Lee and H. Cho, "Experimental Investigation on the Spray Characteristics of a Robotic Spray Paint Gun Used for Car Repaint", International Journal of Mechanical Engineering and Robotics Research, Vol. 11, No. 7, 2022. pp. 494–500. doi: 10.18178/ijmerr.11.7.494-500.

[27] Lin, Z., Zhu, M., Song, C., Liu, T., Yin, C., Zeng, T., and Shao, J., "Effect of annealing on the properties of plasma-enhanced atomic layer deposition grown HfO_2 coatings for ultraviolet laser applications", Journal of Alloys and Compounds, vol. 946, 2023, pp. 1–10. doi: 10.1016/j.jallcom.2023.169443.

[28] L. Zhao, F. Zhang, L. Wang, S. Yan, J. He, and F. Yin, "Effects of post-annealing on microstructure and mechanical properties of plasma sprayed Ti-Si-C composite coatings with Al addition", Surface & Coatings Technology, vol. 416, 2021, pp. 1–9. doi: 10.1016/j.surfcoat.2021.127164.

[29] M. Ashokkumar, D. Thirumalaikumarasamy, T. Sonar, M Ivanov, S. Deepak, P. Rajangam, and R. Barathiraja, "Effect of post-processing treatments on mechanical performance of cold spray coating – an overview", Journal of the Mechanical Behavior of Materials, vol. 32, no. 1, 2023, pp. 1–18. doi: doi:10.1515/jmbm-2022-0271.

[30] S. Roy and P. kumar Mandal. Corrosion Resistance Methods for Stainless Steel: A Review. In New Challenges and Industrial Applications for Corrosion Prevention and Control, 2020, pp. 208–225. doi: 10.4018/978-1-7998-2775-7.ch009.

[31] Praxair and TAFA, "Technical Data Bulletin Arc Spray BondArc® Wire75B®", 2000.

[32] Praxair and TAFA, "Technical Data Bulletin 95MXC ® UltraHard ® Wire Coating", 2000.

[33] Deni Fajar Fitriyana, Samsudin Anis, Abdul Rachman Al Qudus, Mirza Aufa Nugraha Lakuy, Rifky Ismail, Sri Nugroho, Gunawan Dwi Haryadi, Athanasius Priharyoto Bayuseno, & Januar Parlaungan Siregar, "The Effect of Post-Heat Treatment on The Mechanical Properties of FeCrBMnSi Coatings Prepared by Twin Wire Arc Spraying (TWAS) Method on Pump Impeller From 304 Stainless Steel", Journal of Advanced Research in Fluid Mechanics and Thermal Sciences, vol. 93, no. 2, 2022, pp. 138–147. doi: 10.37934/arfmts.93.2.138147.

[34] S. Channappagoudar, K. Aithal, N. Sannayallappa, V. Desai, and P. G. Mukunda, "The influence of the addition of 4.5 wt.% of copper on wear properties of Al-12Si eutectic alloy", Jordan Journal of Mechanical and Industrial Engineering, vol. 9, no. 3, 2015, pp. 217–221. https://jjmie.hu.edu.jo/vol9-3/JJMIE-172-14-01%20Proof%20Reading%20Ok.pdf.

[35] B. D. Bachchhav and K. N. Hendre, "Wear Performance of Asbestos-Free Brake Pad Materials", Jordan Journal of Mechanical and Industrial Engineering, vol. 16, no. 4, 2022, pp. 459–469. https://jjmie.hu.edu.jo/vol-16-4/01-21-22.pdf.

[36] S. K. Aithal, N. R. Babu, H. N. Manjunath, and K. S. Chethan, "Characterization of Al-SiCP Functionally Graded Metal Matrix Composites Developed through Centrifuge Casting Technique", Jordan Journal of Mechanical and Industrial Engineering, vol. 15, no. 5, 2021, pp. 483–490. https://jjmie.hu.edu.jo/vol15-5/08-jjmie_127_20.pdf

[37] M. N. Abijith, A. R. Nair, M. Aadharsh, R. V. Vignesh, R. Padmanaban, and M. Arivarasu, "Investigations on the mechanical, wear and corrosion properties of cold metal transfer welded and friction stir welded aluminium alloy AA2219", Jordan Journal of Mechanical and Industrial Engineering, vol. 12, no. 4, 2018, pp. 281–292. https://jjmie.hu.edu.jo/vol12-4/jjmie_90_18-01.pdf

[38] H. -J. Hoffmann, "Transitions of electrons and holes drive diffusion in crystals, glasses and melts", Materials Science and Engineering Technology, vol. 51, no. 12, 2020, pp. 1578–1614. doi: 10.1002/mawe.201800158.

[39] L. Pawlowski. Post-Spray Treatment. In The Science and Engineering of Thermal Spray Coatings, 2008, pp. 115–165. doi: https://doi.org/10.1002/9780470754085.ch4.

[40] B. Fu, D. He, and L. Zhao, "Effect of heat treatment on the microstructure and mechanical properties of Fe-based amorphous coatings", Journal of Alloys and Compounds, vol. 480, no. 2, 2009, pp. 422–427. doi: https://doi.org/10.1016/j.jallcom.2009.02.107.

[41] J. B. Cheng, X. B. Liang, Y. X. Chen, Z. H. Wang, and B. S. Xu, "High-Temperature Erosion Resistance of FeBSiNb Amorphous Coatings Deposited by Arc Spraying for Boiler Applications", Journal of Thermal Spray Technology, vol. 22, no. 5, 2013, pp. 820–827. doi: 10.1007/s11666-012-9876-5.

[42] P. Daram and C. Banjongprasert, "The influence of post treatments on the microstructure and corrosion behavior of thermally sprayed NiCrMoAl alloy coating", Surface and Coatings Technology, vol. 384, 2020, pp. 1–11. doi: 10.1016/j.surfcoat.2019.125166.

[43] Hongxia Zhou, Chengxin Li, Hao Yang, Xiaotao Luo, Guanjun Yang, Wenya Li, Tanvir Hussain & Changjiu Li, "Pores Structure Change Induced by Heat Treatment in Cold-Sprayed Ti6Al4V Coating", Journal of Thermal Spray Technology, vol. 28, no. 6, 2019, pp. 1199–1211. doi: 10.1007/s11666-019-00882-0.

[44] Y. Ishikawa, J. Kawakita, and S. Kuroda, "Development of corrosion and wear resistant coatings by an improved HVOF spraying process", Materials Science Forum, vol. 475–479, no. 1, 2005, pp. 237–240. doi: 10.4028/0-87849-960-1.237.

[45] H. Nayak, N. Krishnamurthy, and S. R. A, "Development and Adhesion Strength of Plasma-Sprayed Thermal Barrier Coating on the Cast Iron Substrate", International Journal of Integrated Engineering, vol. 13, no. 1, 2021, pp. 47–59. doi: 10.30880/ijie.2021.13.01.006.

[46] A. Bhowmik, A. Wei-Yee Tan, W. Sun, Z. Wei, I. Marinescu, and E. Liu, "On the heat-treatment induced evolution of residual stress and remarkable enhancement of adhesion strength of cold sprayed Ti–6Al–4V coatings", Results in Materials, vol. 7, 2020, pp. 1–9. doi: 10.1016/j.rinma.2020.100119.

[47] Yingchun Xie, Marie-Pierre Planche, Rija Raoelison, Philippe Hervé, Xinkun Suo, Pengjiang He, and Hanlin Liao, "Investigation on the influence of particle preheating temperature on bonding of cold-sprayed nickel coatings", Surface & Coatings Technology, vol. 318, 2017, pp. 99–105. doi: 10.1016/j.surfcoat.2016.09.037.

[48] Guo-Hui Meng, Bang-Yan Zhang, Hong Liu, Guan-Jun Yang, Tong Xu, Cheng-Xin Li, Chang-Jiu Li, "Vacuum heat treatment mechanisms promoting the adhesion strength of thermally sprayed metallic coatings", Surface & Coatings Technology, vol. 344, 2018, pp. 102–110. doi: 10.1016/j.surfcoat.2018.03.010.

[49] Haimin Zhai, Mengjing Ou, Shuai Cui, Wensheng Li, Xinjian Zhang, Bo Cheng, Dongqing He, Xiaosong Li, and Anhui Cai, "Characterizations the deposition behavior and mechanical properties of detonation sprayed Fe-based amorphous coatings," Journal of Materials Research and Technology, vol. 18, 2022, pp. 2506–2518. doi: https://doi.org/10.1016/j.jmrt.2022.03.140.

[50] P.R. Rajendran, T. Duraisamy, S.R. Chidambaram, A. Mohankumar, S. Ranganathan, G. Balachandran, K. Murugan K, L. Renjith, "Optimisation of HVOF Spray Process Parameters to Achieve Minimum Porosity and Maximum Hardness in WC-10Ni-5Cr Coatings", Coatings, vol. 12, no. 3, 2022. pp. 1–20. doi: 10.3390/coatings12030339.

[51] K. Palanisamy, S. Gangolu, and J. M. Antony, "Effects of HVOF spray parameters on porosity and hardness of 316L SS coated Mg AZ80 alloy", Surface and Coatings Technology, vol. 448, 2022, pp. 1–13. doi: https://doi.org/10.1016/j.surfcoat.2022.128898.

[52] R. V Prasad, R. Rajesh, D. Thirumalaikumarasamy, S. Vignesh, and S. Sreesabari, "Sensitivity analysis and optimisation of HVOF process inputs to reduce porosity and maximise hardness of WC-10Co-4Cr coatings", Sādhanā, vol. 46, no. 149, 2021, pp. 1–23. doi: 10.1007/s12046-021-01667-4.

[53] O. V. Sobol', A. A. Meylekhov, V. A. Stolbovoy, and A. A. Postelnyk, "Structural Engineering Multiperiod Coating ZrN/MoN", Journal of Nano- and Electronic Physics, vol. 8, no. 3, 2016, pp. 1–4, 2016, doi: 10.21272/jnep.8(3).03039.

[54] G. J. Li, J. Li, and X. Luo, "Effects of post-heat treatment on microstructure and properties of laser cladded composite coatings on titanium alloy substrate", Optics & Laser Technology, vol. 65, 2015, pp. 66–75. doi: 10.1016/j.optlastec.2014.07.003.

[55] J. Hu, J. Jie, L. Hui, Y. Xian, X. Hongbin, J. Yan, M. Chaoping, D. Qingshan, and G. Ning, "Effect of Annealing Treatment on Microstructure and Properties of Cr-Coatings Deposited on AISI 5140 Steel by Brush-Plating", Coatings, vol. 8, no. 5, 2018, pp. 1–10. doi: 10.3390/coatings8050193.

[56] F. Zhang, C. Li, S. Yan, J. He, and F. Yin, "Improving hardness and toughness of plasma sprayed Ti–Si–C nano-composite coatings by post Ar-annealing", Ceramics International, vol. 47, no. 3, 2021, pp. 3173–3184. doi: https://doi.org/10.1016/j.ceramint.2020.09.154.

[57] H. Dhiflaoui, N. Ben Jaber, F. S. Lazar, J. Faure, A. B. C. Larbi, and H. Benhayoune, "Effect of annealing temperature on the structural and mechanical properties of coatings prepared by electrophoretic deposition of TiO_2 nanoparticles", Thin Solid Films, vol. 638, 2017, pp. 201–212. doi: https://doi.org/10.1016/j.tsf.2017.07.056.

[58] R. Kosasih, M.M. Suliyanti, D. Priadi, W. Usni, "Optimization of AlTi PLD coating by increasing Ti content, N2 and Annealing which used for SKD61 pins in aluminum die casting", Journal of Materials Exploration and Findings, vol. 2, no. 2, 2023, pp. 1–15. doi: 10.7454/jmef.v2i2.1027.

[59] Robert C. Tucker, Jr., ASM Handbook, Volume 5A: Thermal Spray Technology, ASM Thermal Spray Society, 2004.

[60] M. Arana, E. Ukar, I. Rodriguez, A. Iturrioz, and P. Alvarez, "Strategies to Reduce Porosity in Al-Mg WAAM Parts and Their Impact on Mechanical Properties", Metals (Basel)., vol. 11, no. 3, 2021, pp. 1–18. doi: 10.3390/met11030524.

[61] P. Gao, B. Chen, S. Zeng, Z. Yang, Y. Guo, M. Liang, T. Xu, and J. Li, "Effect of Vacuum Annealing on the Nickel-Based Coatings Deposited on a CGI Cast Iron through Atmospheric Plasma Spraying", Metals (Basel)., vol. 10, no. 7, 2020, pp. 1–18. doi: 10.3390/met10070963.

[62] R. A. Seraj, A. Abdollah-zadeh, S. Dosta, H. Canales, H. Assadi, and I. G. Cano, "The effect of traverse speed on deposition efficiency of cold sprayed Stellite 21", Surface and Coatings Technology, vol. 366, 2019, pp. 24–34. doi: https://doi.org/10.1016/j.surfcoat.2019.03.012.

[63] Can Chen, Xuemei Song, Wei Li, Wei Zheng, Heng Ji, Yi Zeng, Ying Shi, "Relationship between microstructure and bonding strength of yttria-stabilized zirconia thermal barrier coatings", Ceramics International, vol. 48, no. 4, 2022, pp. 5626–5635. doi: https://doi.org/10.1016/j.ceramint.2021.11.107.

[64] Q. Zhu, Y. Liu, W. Cong, D. Chang, Q. Fan, F. Cao, T-G. Wang, "The Effect of Vacuum Annealing Temperature on the Properties of AlCrTiSiN Coating Prepared by Arc Ion Plating", Coatings, vol. 12, no. 3, 2022, pp. 1–18. doi: 10.3390/coatings12030316.

[65] S. Lavrys, I. Pohrelyuk, J. Padgurskas, and K. Shliakhetka, "Improving Wear Resistance of Highly Porous Titanium by Surface Engineering Methods", Coatings, vol. 13, no. 10, 2023, pp. 1–14. doi: 10.3390/coatings13101714.

[66] J. E. Kisel and G. V Guryanov, "Wear Resistance of Composite Coatings Based on Iron Alloys", IOP Conference Series: Materials Science and Engineering, vol. 450, 2018, pp. 1–5. doi: 10.1088/1757-899X/450/3/032047.

[67] R. A. Al-Samarai, Y. Al-Douri, and Haftirman, "Porosity effect on the tribological properties of Al-Si alloys for diamond-like carbon coating of cold sprayed", Journal of King Saud University-Engineering Sciences, vol. xx, no. xx, 2021, pp. 1–11. doi: 10.1016/j.jksues.2021.08.009.

[68] B. M. Moshtaghioun, D. Gomez-Garcia, A. Dominguez-Rodriguez, and R. I. Todd, "Abrasive wear rate of boron carbide ceramics: Influence of microstructural and mechanical aspects on their tribological response", Journal of the European Ceramic Society, vol. 36, no. 16, 2016, pp. 3925–3928. doi: 10.1016/j.jeurceramsoc.2016.06.029.

[69] V. R. Gumen and V. V. Kovriga, "Development of roughness and decrease in hardness of abrasive wear surface in various types of polyethylene. Part I.", Plasticheskie massy, vol. 1, no. 11–12, 2022, pp. 26–28. doi: 10.35164/0554-2901-2021-11-12-26-28.

[70] P.V.C.S. Rao, A.S. Devi, and K.G.B. Kumar, "Influence of melt treatments on dry sliding wear behavior of hypereutectic Al-15Si-4Cu cast alloys", Jordan Journal of Mechanical and Industrial Engineering., vol. 6, no. 1, 2012, pp. 55–61. https://jjmie.hu.edu.jo/files/v6n1/JJMIE-107-11.pdf

[71] D. Dinakaran, S. Sampathkumar, and J. S. Mary, "Real Time Prediction of Flank Wear by Neuro Fuzzy Technique in Turning", Jordan Journal of Mechanical and Industrial Engineering., vol. 4, no. 6, 2010, pp. 725–732. https://jjmie.hu.edu.jo/files/v4n6/7.pdf.

[72] R. J. Mustafa, "Abrasive Wear of Continuous Fibre Reinforced Al And Al-Alloy Metal Matrix Composites", Jordan Journal of Mechanical and Industrial Engineering., vol. 4, no. 2, 2014, pp. 246–255. https://jjmie.hu.edu.jo/files/v4n2/JJMIE-71-08_Revised%20modified.pdf.

[73] Y. Zhang, Y. Ma, M. Duan, G. Wang, and Z. Li, "The Improvement of the Wear Resistance of T15 Laser Clad Coating by the Uniformity of Microstructure", Lubricants, vol. 10, no. 10, 2022, pp. 1–14. doi: 10.3390/lubricants10100271.

[74] D. B. Buitkenov, B. K. Rakhadilov, Z. B. Sagdoldina, and D. Erbolatuly, "Reserach of the mechanic-tribological characteristics of Ti_3SiC_2/TiC coatings after annealing", Eurasian Journal of Physics and Functional Materials, vol. 4, no. 1, 2020, pp. 86–92. doi: 10.29317/ejpfm.2020040109.